



Title	Effects of Design and Operation Variables on the Autothermic Reactor
Author(s)	KASHIKI, Isamu; MIKI, Masayuki; SUZUKI, Akira; SAKAI, Makoto
Citation	北海道大學水産學部研究彙報, 31(3), 265-275
Issue Date	1980-08
Doc URL	http://hdl.handle.net/2115/23726
Type	bulletin (article)
File Information	31(3)_P265-275.pdf



[Instructions for use](#)

Effects of Design and Operation Variables on the Autothermic Reactor

Isamu KASHIKI*, Masayuki MIKI*, Akira SUZUKI*
and Makoto SAKAI*

Abstract

Effects of the heat transfer between the catalyst bed and the internal heat exchanger, the length of the catalyst bed, the bypass and the heater used for adjusting the temperature profile of the catalyst bed, and the flow rate of the performance of the autothermic reactor, and the role of pressure played in varying the reactor condition are discussed by numerical methods of analysis. The operation under lower temperatures using much catalyst with less heat transfer per m^3 catalyst, at the greatest possible flow rate is the preferable outcome from a commercial viewpoint.

Introduction

In a previous paper¹⁾, we have discussed the behavioral characteristics, stability and optimization of four autothermic reactors — two 2-pass (counter-flow and parallel-flow) reactors and two 3-pass (double-pipe and mixed-flow) reactors. This paper is concerned with the effects of design and operation variables on the performance and the role of pressure for the 2-pass counter-flow reactor shown in Fig. 1. To be simple and clear, we do not refer to other types of reactors, however it should be understood that similar results are obtainable therefrom. Baddour *et al.*²⁾ also have discussed the effects of some variables, but our treatment is different from theirs in paying special attention to follow the order of cause and effect.

Method of Mathematical Treatment

For ease in problem solving, the following assumptions are made without much loss of generality.

1. Steady state.
2. Plug flow with no axial heat transfer.
3. No radial heat resistance except at the tube wall and the adjacent films.
4. No heat gain from or loss to the surroundings.

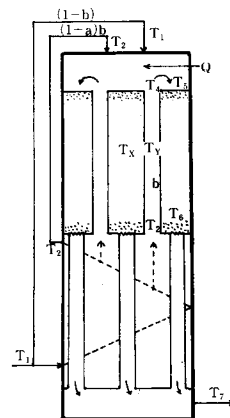


Fig. 1. Schematic representation of the 2-pass counter-flow reactor

* Laboratory of Chemical Engineering, Faculty of Fisheries, Hokkaido University
(北海道大学水産学部化学工学講座)

5. Constant specific heat of reacting mass as a whole, irrespective of the composition and temperature.
6. Unimolecular reaction $A \xrightleftharpoons[k_{-1}]{k_1} B$, $k_1/k_{-1}=K$ occurring, with the heat of reaction, ΔH and the energy of activation, E .
7. Overall heat transfer coefficient proportional to the 0.75th power of the mass velocity.
8. Constant temperature of the inlet reactant ($\theta_0=\text{constant}$).

Under these assumptions, following nine simultaneous equations should hold for the 3-pass mixed-flow reactor, and, if β_2 vanishes, and hence θ_2 equals θ_3 , they represent the two-pass counter-flow reactor.

$$\theta_2 = [\gamma / \{b + \gamma/2(1-b)\}] \cdot \theta_7 \tag{1}$$

$$\theta_6 = \theta_7 + b\theta_2 \quad (= \Delta X + \theta_0 + b\theta_2) \tag{2}$$

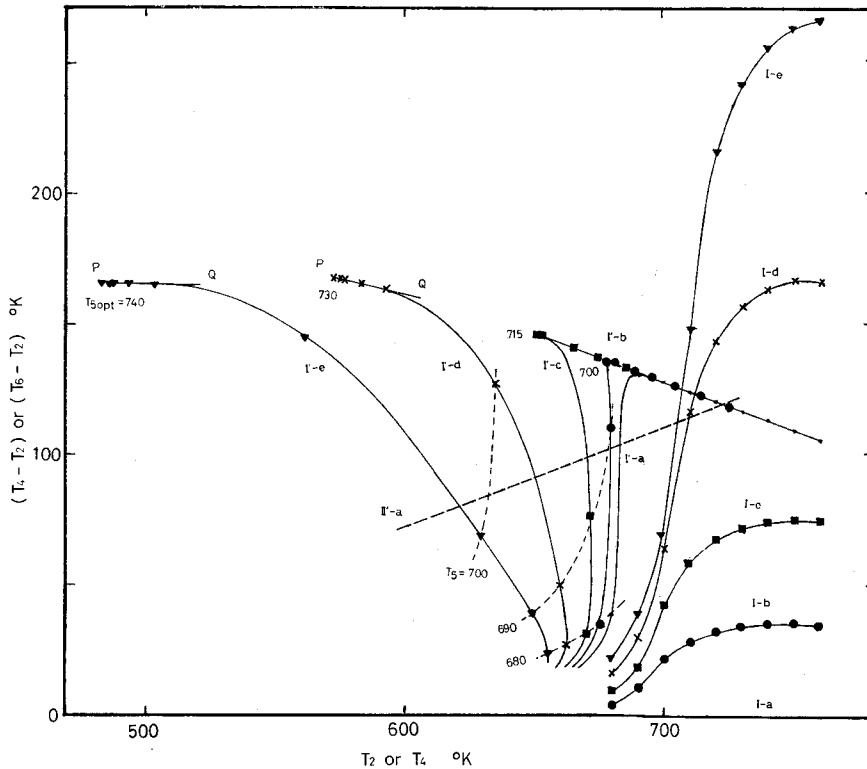


Fig. 2. Effect of heat transfer between the catalyst bed and the cooling pipes. ($F=920$, $C_0C_p=47.2$, $C_0=4.44$, $C_i=4.20$, $l=5$, $a=b=1$, $\Delta H=-7000$, $E=40000$, $k_0=0.5 \cdot 10^{14}$, $K_0=0.4735 \cdot 10^{-2}$) Curved line I refers to the relation between T_4 and $(T_4 - T_2)$, I' , to the relation T_2 and $(T_6 - T_2)$ from Eqs. (6), (7), (8), whereas straight line II' denotes the relation between T_2 and $(T_6 - T_2)$ from Eqs. (1), (2). $U_1S_1=0$ for I-a, I'-a; =2875 for I-b, I'-b; =5750 for I-c, I'-c; =11500 for I-d, I'-d; =17250 for I-e, I'-e.

$$\theta_5 = ab\theta_4 + (1-a)b\theta_2 + \theta_Q \quad (3)$$

$$X - X_i = ab(\theta_Z - \theta_Y) + \theta_X - b\theta_2 - \theta_Q \quad (4)$$

$$\Delta X = X_f - X_i = \theta_7 - \theta_Q \quad (5)$$

$$\frac{d\theta_X}{d\lambda} = V' - \beta_1(\theta_X - \theta_Y) - \beta_2(\theta_X - \theta_Z) \quad (6)$$

$$\frac{d\theta_Y}{d\lambda} = \frac{\beta_1}{ab}(\theta_X - \theta_Y) \quad (7)$$

$$\frac{d\theta_Z}{d\lambda} = \frac{\beta_2}{ab}(\theta_X - \theta_Z) \quad (8)$$

$$V' = \exp\{-\varepsilon/(\theta_0 + \theta_X)\} (1 - X - X/[K_0 \exp\{\delta/(\theta_0 + \theta_X)\}]) \quad (9)$$

where $V' = V/k_0 C_0$

and the boundary conditions for (6), (7) and (8) are

$$\lambda = 0; \theta_X = \theta_5, \theta_Y = \theta_4, \theta_Z = \theta_2$$

$$\lambda = \lambda_0; \theta_X = \theta_6, \theta_Y = \theta_Z = \theta_3$$

The method of solution has been given in the previous paper.

The Result and Discussion

Effect of Heat Transfer between the Catalyst Bed and the Cooling Tubes in the Internal Heat Exchanger

The parameters, S_1 and S_2 are design variables, but U_1 and U_2 depend upon flow rates and so not fundamental variables. $U_1 S_1$ and $U_2 S_2$ represent heat transfer capacity and affect β_1 and β_2 but do not affect γ . Fig. 2 shows the effect of $U_1 S_1$ on the performance of the 2-pass counter-flow autothermic reactor, from which it can be seen that:

(1) If there is no heat transfer, in which case the reactor reduces to an adiabatic one, the reactor has no unstable zone as proposed by van Heerden³, because the slope of any tangent to the curved line I'-a is at least not less than null. However, in the presence of the

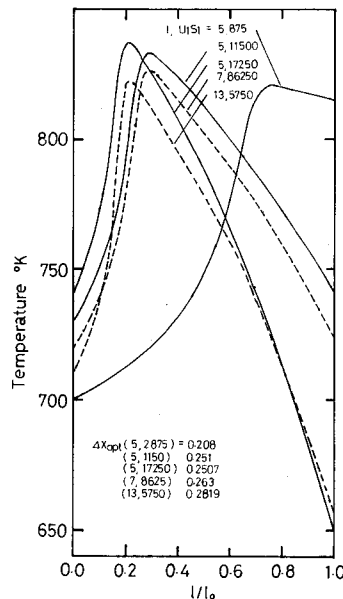


Fig. 3. Optimum temperature profiles of the catalyst bed at different catalyst bed lengths and at different degrees of heat transfer in the autothermic part.

($C_0 C_p = 47.2$, $C_0 = 4.44$, $C_i = 4.20$, $a = b = 1$, $\Delta H = -7000$, $E = 40000$, $k_0 = 0.5 \cdot 10^{-4}$, $K_0 = 0.4735 \cdot 10^{-2}$)

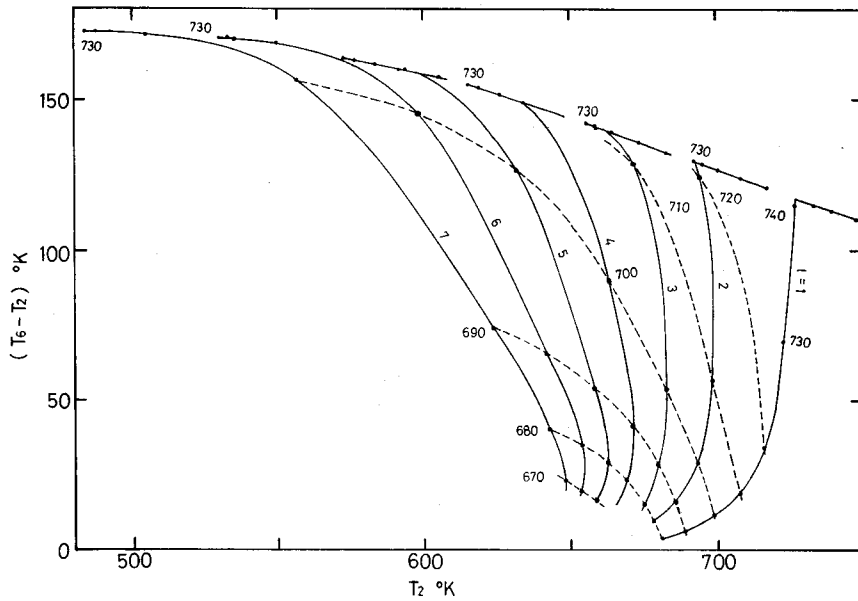


Fig. 4. Effect of catalyst bed length. ($F=920$, $C_0C_p=47.2$, $C_0=4.44$, $C_i=4.20$, $U_1S_1=11500$, $a=b=1$, $\Delta H=-7000$, $E=40000$, $k_0=0.5 \cdot 10^{-2}$, $K_0=0.4735 \cdot 10^{-2}$ Catalyst bed length; 1, 2, 3, 4, 5, 6, 7.

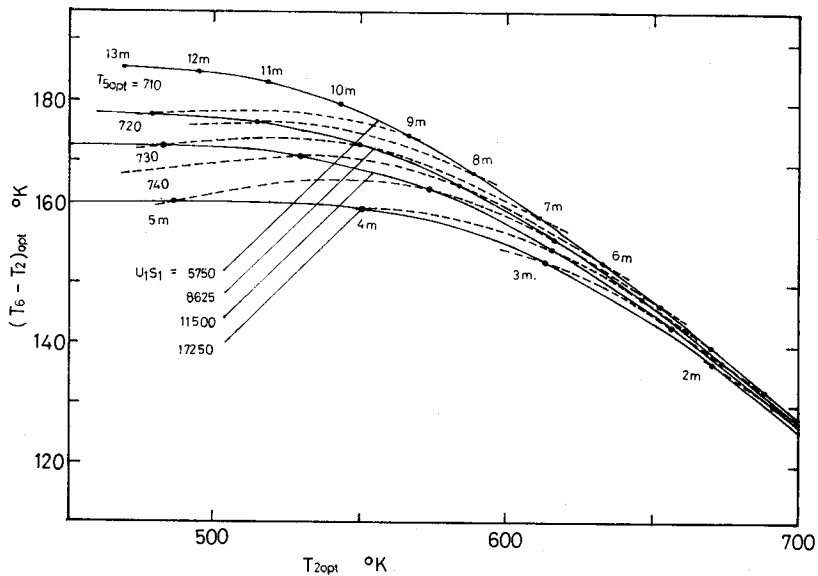


Fig. 5. Effect of catalyst bed length at different U_1S_1 's. (The condition is the same as in Fig. 4 except for the values of U_1S_1 's, which take the values of 5750, 8675, 11500, 17250.) Catalyst bed length; 2, 3, 4, 5, 6, 7, 8, 9, 10, 11, 12, 13.

external heat exchanger, the unstable zone based on our criterion does exist, as can be seen from the relation between the curved line I'-a and the straight line II'-a¹).

(2) With the presence of the heat transfer, the van Heerden unstable zone appears, and as the heat transfer increases, both van Heerden and our unstable zones increase, the curve I' which expresses the solution of Eqs. (6), (7) and (8) on the $T_2-(T_6-T_2)$ plane takes a sigmoidal shape whose upper left part projects sharper, T_2 falls, T_{5opt} rises, and the slope of the curved line at the upper stable zone, PQ , tends to null.

(3) Provided that the catalyst bed length is held constant, a condition which gives maximum ΔX_{opt} exists at some U_1S_1 value.

The optimum temperature profiles of the catalyst bed at different U_1S_1 's are depicted in Fig. 3.

Effect of Catalyst Bed Length

The catalyst bed length, l_0 , is a design variable and affects only λ_0 and does

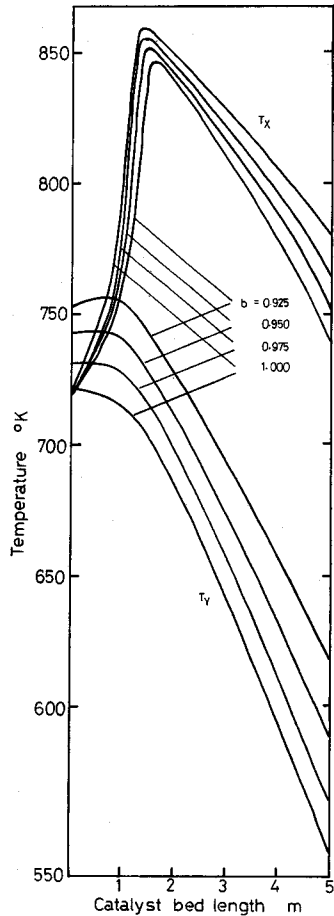


Fig. 6. Temperature profiles of the catalyst bed with or without bypass (b). ($F=920, C_oC_p=47.2, C_o=4.44, C_i=4.20, U_1S_1=11500, a=1, l=5, \Delta H=-7000, E=14000, k_o=0.5 \cdot 10^{14}, K_o=0.4735 \cdot 10^{-2}$) $b=1.000, 0.975, 0.950, 0.925$.

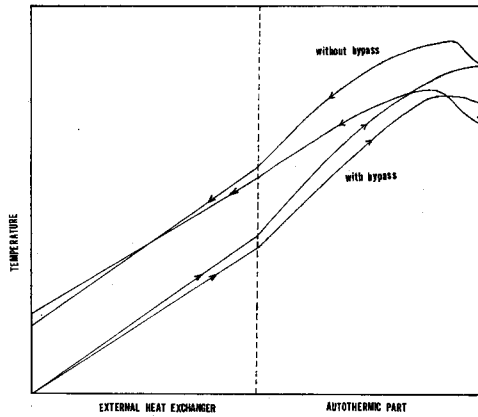


Fig. 7. Temperature profile of the whole reactor when the bypass (b) is used. Left half refers to the external heat exchanger and right half, the catalyst bed.

Fig. 6. Temperature profiles of the catalyst bed with or without bypass (b). ($F=920, C_oC_p=47.2, C_o=4.44, C_i=4.20, U_1S_1=11500, a=1, l=5, \Delta H=-7000, E=14000, k_o=0.5 \cdot 10^{14}, K_o=0.4735 \cdot 10^{-2}$) $b=1.000, 0.975, 0.950, 0.925$.

not affect β_1 and γ . The effect of increased catalyst bed length at constant U_1S_1 , is somewhat similar to the effect of increased heat transfer at constant catalyst bed length. The differences are that the conversion increases at a decelerating rate and no maximum ΔX_{opt} exists, and T_{5opt} falls, with an increased bed length (Fig. 4). As can be seen from Fig. 5, $(U_1S_1)_{opt}$ which gives maximum ΔX_{opt} , or $(T_2 - T_6)_{opt}$, at the constant catalyst bed length, decreases with the increase in catalyst bed length. In short, the effect of prolonged catalyst bed length is to increase conversion while keeping lower catalyst temperature. The optimum catalyst temperature at different bed lengths are shown in Fig. 3.

In the commercial reactor, longer catalyst bed implies more catalyst volume, more heat loss to the surroundings and longer equipment, and hence more capital investment, whereas less heat transfer between the catalyst bed and the internal heat exchanger brings about less capital investment. The cost of the reactor is said commonly to be only about ten percent of the total capital cost summed up within battery limit, while the more catalyst volume and the lower catalyst temperature mean usually safer operation and longer catalyst life. The decision upon

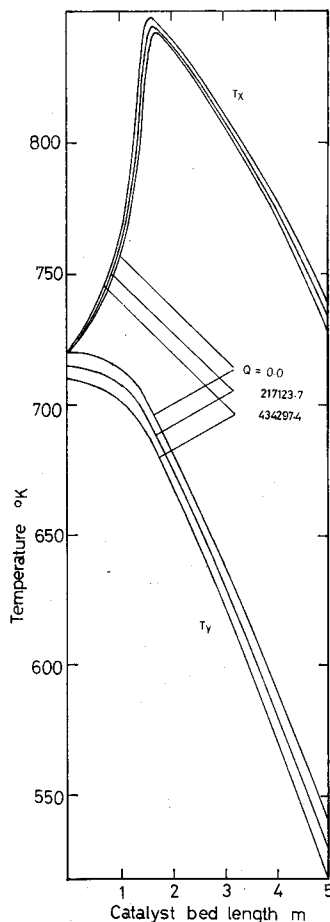


Fig. 8. Temperature profiles of the catalyst bed with or without heater. ($F=920$, $C_0C_p=47.2$, $C_0=4.44$, $C_i=4.20$, $U_1S_1=11500$, $l=5$, $a=b=1$, $\Delta H=-7000$, $E=40000$, $k_0=0.5 \cdot 10^{14}$, $K_0=0.4735 \cdot 10^{-2}$) $Q=0$, 217123.7, 434297.4.

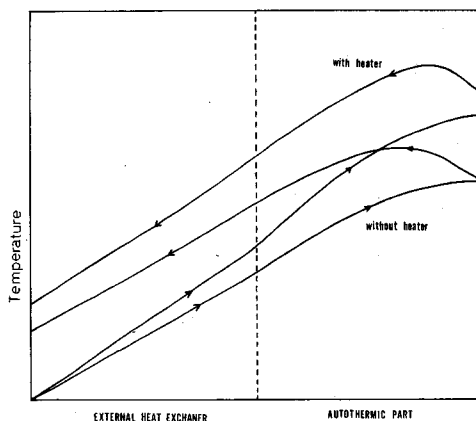


Fig. 9. Temperature profile of the whole reactor when the heater is used. Left half refers to the external heat exchanger and right half, the catalyst bed.

the catalyst bed length depends upon their compromise which places usually more emphasis on conversion, safety and life of catalyst.

Effect of Bypass and Heater

As can be seen from the mathematical model, the bypass (*b*) connecting the input reactant line to the catalyst bed inlet and the heater mounted at the catalyst bed inlet affect the behavior of the autothermic part and the external heat exchanger through the operation variable, *b* and θ_2 . Fig. 6 which depicts the temperature profiles of the catalyst beds with or without a bypass, discloses characteristic features of interest that, with a bypass, T_4 is higher than T_5 , and the curve representing T_Z has a maximum at the intersection of the lines expressing T_X and T_Y . In Fig. 7 which pictures the temperature profile of the whole reactor, T_2 , T_4 , T_5 , T_6 and the whole temperature profile tend to fall, with decreasing *b*, and, because the bypass is always used for adjusting the temperature distribution, the conversion, ΔX , increases.

By contrast, in Fig. 8 which displays the temperature profiles with or without a heater, it is seen that, with a heater, T_5 is higher than T_4 and the curve representing T_Y has positive slope and no maximum at any place, and, as can be seen from Fig. 9, T_2 , T_4 , T_5 , T_6 and the whole catalyst temperature rise, with increased heating, and the conversion, ΔX , increases as a result of adjusted temperature distribution.

Another bypass (*a*) connecting the exit of the reactant from the external heat exchanger to the inlet of the catalyst bed (Fig. 1), unlike the bypass (*b*), does not alter the reactant throughput in the external heat exchanger. Its function is much like the bypass (*b*) except less effective and less frequently used, and therefore not dealt with in this paper.

Effect of Feed Rate

Like the bypass (*b*) and the heater, feed rate or throughput is also an operation variable and affects the performance of the external heat exchanger and the autothermic part through changing the values of γ , λ_0 , and further, β_i , because U_i depends on *F*. Fig. 10 shows that increased feed rates at constant T_5 , always induce levelling off of the temperature profiles, while Fig. 11 discloses an interesting

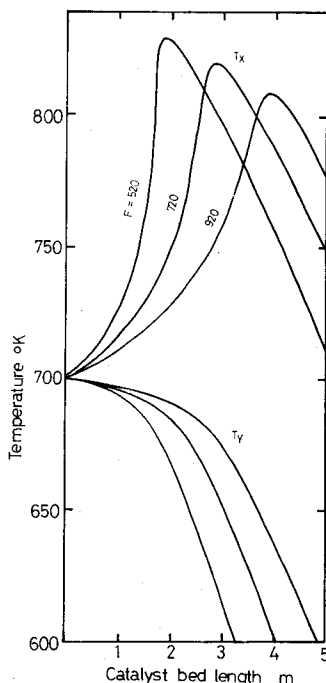


Fig. 10. Temperature profiles of the catalyst bed having the same T_5 at different flow rates. ($C_0 C_p = 47.2$, $C_0 = 4.44$, $C_i = 4.20$, $U_1 S_1 = 6.0 \cdot F^{0.75} \cdot 11.5$, $a = b = 1$, $l = 5$, $\Delta H = -7000$, $E = 40000$, $k_0 = 0.5 \cdot 10^{14}$, $K_0 = 0.4735 \cdot 10^{-2}$) $F = 520, 720, 920$.

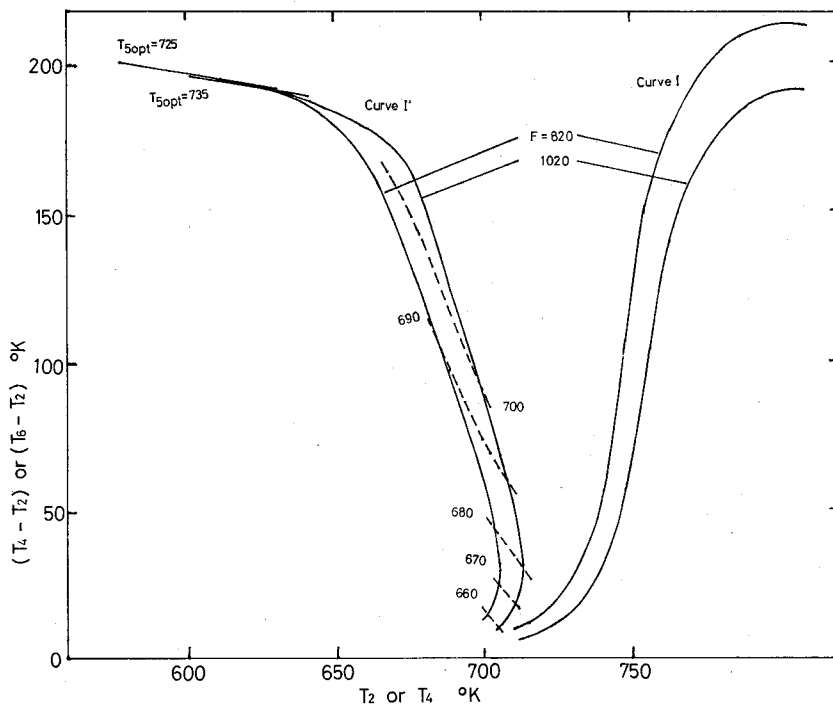


Fig. 11. Effect of flow rate. ($C_0 C_p = 47.2$, $C_0 = 4.44$, $C_i = 4.44$, $U_1 S_1 = 6.0 \cdot F^{0.75} \cdot 11.5$, $a = b = 1$, $l = 5$, $\Delta H = -7000$, $E = 40000$, $k_0 = 0.5 \cdot 10^{14}$, $K_0 = 0.4735 \cdot 10^{-2}$) $F = 820, 1020$.

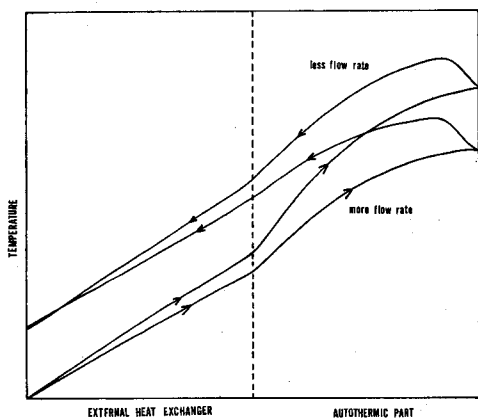


Fig. 12. Temperature profile of the whole reactor at different flow rates. Left half refers to the external heat exchanger and right half, the catalyst bed.

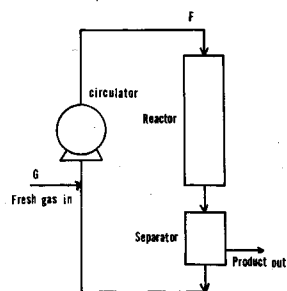


Fig. 13. Flow chart of the synthesis loop applied to the manufactures of ammonia and methanol.

fact that all the curves representing the relation between T_2 and $(T_6 - T_2)$ or ΔX , pass practically the same line at the upper stable zone, irrespective of feed rate. If the effect of feed rate on the external heat exchanger is taken into consideration, the temperature profiles of the whole reactor at different feed rates can be depicted schematically as shown in Fig. 12. Thus the increase in feed rate implies invariable approach to instability notwithstanding slight increases in conversion, and this explains the so-called "blow out", or sudden drop of catalyst temperature which occurs when too much feed is supplied.

Role of Pressure

We have assumed, up to this point, C_0 , and accordingly, the reaction pressure is constant, which is, of course, not the real situation. There are two important cases in the application of the autothermic reactor which deserve special attention regarding the role of pressure, of the syntheses of ammonia and methanol, their characteristic flow chart, in common, being shown in Fig. 13.

When the catalyst is new and its activity is high, the reaction progresses rapidly, and much product is produced and taken out from the reaction loop, therefore, provided that the reactant feed rate to the loop, G , is held constant, the pressure tends to fall. However, a lowered pressure gives rise to a decrease in the reactor performance, through lowered circulator capacity, FC_0 , which is proportional to the pressure, and through slow-down of the reaction velocity which is proportional to C_0 . Thus there appears a new steady condition, as a result of their compromise, at a lower pressure.

It is interesting to note that, in theory, another steady condition can be thought of without lowering the pressure, by raising the catalyst temperature and thereby bringing about slow-down of the reaction velocity, and still other innumerable steady conditions, by combining pressure lowering and temperature raising, which, in practice, never occur spontaneously because of less mechanical and thermodynamical stabilities.

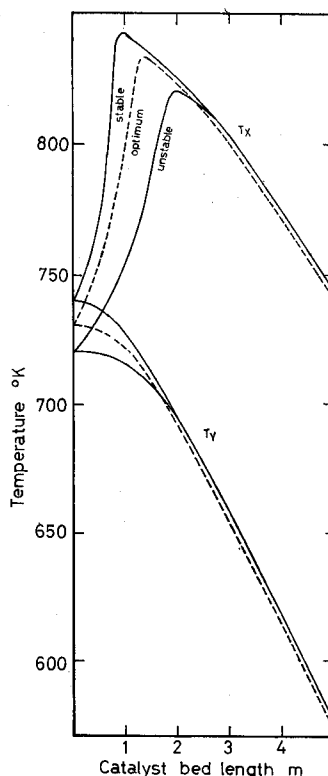


Fig. 14. Temperature profiles of the catalyst bed near optimum conversion. ($F=920$, $C_0C_p=47.2$, $C_0=4.44$, $C_i=4.20$, $U_1S_1=11500$, $l=5$, $a=b=1$, $\Delta H=-7000$, $E=40000$, $k_0=0.5 \cdot 10^{14}$, $K_0=0.4735 \cdot 10^{-2}$) The dashed line shows the one at the optimum condition. The upper solid line refers to a stable condition, whereas the lower one, an unstable condition.

Mathematically, in the simultaneous equations, (1) through (9), C_0 is proportional to pressure, and, by assumption, U_1 , U_2 and U_X are proportional to the 0.75th power of C_0 , so that β_1 , β_2 and γ are inversely proportional to the 0.25th power of pressure, and their increase due to the lowered pressure induces θ_2 , θ_3 , θ_4 , θ_5 , θ_6 and the whole catalyst temperature profile to rise, and consequently, the conversion, ΔX , and the space time yield, $FC_0\Delta X$ to decrease.

As the catalyst deteriorates, the pressure gradually increases and finally reaches the prescribed value, and the flow rate must be reduced thereafter until shut-down.

Catalyst Temperature Profile near Optimum Conversion

In Fig. 14, the upper solid curve refers to a stable condition, and the lower, for an unstable condition. They are nearly the same except at the upstream part, which suggests that they are differentiable most sharply by measuring the temperature there. Besides, this portion senses possible disturbances earliest. This explains the reason why it is used primarily as a measuring point for automation.

Nomenclature

- A : Reactant
- a : Fraction of the reactant which enters the internal heat exchanger to that which leaves the external heat exchanger
- B : Product
- b : Fraction of the reactant which passes through the external heat exchanger to total input reactant
- C_0 : Concentration or density of the input and the reacting mass at any position, in kg-mol/m³
- C_i : Concentration of the product in the input, in kg-mol/m³
- C_f : Concentration of the product in the output, in kg-mol/m³
- C_p : Specific heat of reactant (and also, product), in kcal/mol, °C
- E : Energy of activation, in kcal/kg-mol
- F : Flow rate per unit catalyst cross-sectional area perpendicular to the flow direction, in m³/m², h
- G : Flow rate per unit catalyst cross-sectional area of the input to the synthesis loop, in m³/m², h
- ΔH : Heat of reaction assumed positive for an endothermic reaction, in kcal-kg/mol
- K_0 : Apparent equilibrium constant at 0°K
- k_0 : Preexponential factor of the unimolecular rate constant, in h⁻¹
- l : Distance measured from the inlet of the catalyst bed along the flow, in m
- Q : Heat input from the surroundings per unit catalyst cross-sectional area per unit time at the inlet of the catalyst bed, in kcal/m², h
- R : Gas constant
- S : Heat transfer area per unit cross-sectional area and per unit length of the catalyst bed, in m²/m³
- S_1 : S between the catalyst bed and the cooling pipe in the counter-flow internal heat exchanger, in m²/m³
- S_2 : S between the catalyst bed and the cooling pipe in the parallel-flow

- internal heat exchanger, in m^2/m^3
- S_X : Heat transfer area of the external heat exchanger per unit cross-sectional area of the catalyst bed, in m^2/m^2
- T_i : Temperature at point i or realm i , in $^\circ\text{K}$
- U_1 : Overall heat transfer coefficient between the catalyst bed and the counter-flow cooling pipe in the internal heat exchanger, in $\text{kcal}/\text{m}^2, \text{h}, ^\circ\text{K}$
- U_2 : Overall heat transfer coefficient between the catalyst bed and the parallel-flow cooling pipe in the internal heat exchanger, in $\text{kcal}/\text{m}^2, \text{h}, ^\circ\text{K}$
- U_X : Overall heat transfer coefficient at the external heat exchanger, in $\text{kcal}/\text{m}^2, \text{h}, ^\circ\text{K}$
- V : Unimolecular reaction rate, in $\text{kg}\text{-mol}/\text{m}^3, \text{h}$
- V' : Dimensionless unimolecular reaction rate, V/k_0C_0
- X_i : Mole fraction of the product at the reactor inlet, C_i/C_0
- X_f : Mole fraction of the product at the reactor outlet, C_f/C_0
- ΔX : Conversion, $X_f - X_i$
- β_i : Dimensionless heat transfer coefficient, $U_i S_i / (k_0 C_0 C_p)$
- γ : Dimensionless heat transfer coefficient, $U_x S_x / (FC_0 C_p)$
- δ : Constant, C_p/R
- ε : Constant, $C_p E / R(-\Delta H)$
- λ : Dimensionless catalyst bed length, $k_0 l / F$
- θ_i : Dimensionless temperature assuming $T_1=0$, $C_p(T_i - T_1) / (-\Delta H)$
- θ_0 : Absolute dimensionless temperature corresponding to T_1 , $C_p T_1 / (-\Delta H)$
- θ_Q : Dimensionless temperature rise due to the heating from outside, $Q / FC_0 C_p$

Subscript opt refers to the condition which gives maximum conversion among the solutions of Eqs. (6), (7) and (8) (point P in Fig. 2).

References

- 1) Kashiki, I, Miki, M., Suzuki, A. and Sakai, M. (1979). Analysis of autothermic reactors with external heat exchangers. *Bull. Fac. Fish. Hokkaido Univ.* **30**(4), 323-332.
- 2) Baddour, R.F., Brian, P.L.T., Logeais, B.A. and Eymery, J.P. (1965). Steady-state simulation of an ammonia synthesis converter. *Chem. Eng. Sci.* **20**, 281-292.
- 3) van Heerden, C. (1953). Autothermic process, properties and reactor design. *Ind. Eng. Chem.* **45**, 1242-1247.